25th ABCM International Congress of Mechanical Engineering
October 20-25, 2019, Uberlândia, MG, Brazil

COB-2019-1805
INTENSIFICATION OF POOL BOILING HEAT TRANSFER BY USING MICRO-FIN SURFACES

Igor Seicho Kiyomura[1]
igorseicho@gmail.com
Reinaldo Rodrigues de Souza[1]
reisartre@gmail.com
Elaine Maria Cardoso[1],
elaine.cardoso@unesp.br
[1]UNESP – São Paulo State University, Post-Graduation Program in Mechanical Engineering, Av. Brasil, 56, 15385-000, Ilha Solteira, SP, Brazil.

Abstract. *The need for more efficient and compact heat exchangers, especially in microelectronics, and products with high thermal load has been motivating the research on new technics for increasing the boiling heat transfer. The heated surface can be modified by using micro-fins that enlarge the effective area for heat transfer. In this context, this work aims to analyze modified heating surfaces consisting of micro-fin array surfaces. All surfaces were submitted to metallographic (scanning electron microscopy), wettability and pool boiling tests by using DI-water as working fluid (at saturated conditions). The presence of the micro-fins increases the contact area with liquid leading to a heat transfer augmentation as compared to the plain surface.*

Keywords: *microstructure, micro-fin surface, pool boiling, heat transfer coefficient.*

1. INTRODUCTION

Recent developments in microsystems have made it possible to increase the processing capacity of various electronic devices with a continuous reduction in their size. However, due to the technology advance and the growth of processing capacity, the heat dissipated per unit area in such devices increased significantly (Demir et al., 2014).

The motivation for conducting research on the boiling phenomenon is due to the high heat transfer rates (2.5 - 100 kW/m²) for low values of surface overheating (5 - 15 °C), when compared to the other heat transfer processes (Bejan, 1984). One promising way to enhance the heat transfer coefficient (HTC) and the critical heat flux (CHF) is modifying the heating surface morphology by using coating process or machining techniques and chemicals processes.

Microstructured surfaces, *i.e.,* surfaces with the presence of micro-pillars on the surface, provide small perturbations in the liquid, affecting the vapor bubbles dynamic. These structures increase the heating surface area and change the fluid flow. Micro-fins can have different shapes and sizes and can be arranged in different patterns to improve heat transfer (Liang and Mudawar, 2019). Dong et al. (2014) compared the performance of silicon surfaces with microstructures and nanostructures. Surfaces with microstructures showed higher density of active nucleation sites than those with nanostructures. However, nanostructures surfaces can promote the vapor bubbles departure by decreasing its diameter, which can also prevent the formation of a vapor blanket at high heat fluxes.

Nirgude and Sahu (2017) investigated the pool boiling heat transfer performance of different surfaces with orthogonally intersecting tunnel structured by using water or isopropyl alcohol as working fluids. The experimental study revealed that the tunnel structure enhances the liquid transport network to active nucleation sites on the surface, improving the liquid/vapor interaction on surface and delaying the dryout occurrence.

Cao et al. (2018) studied different types of modified surfaces. The authors analyzed micro-finned silicon surfaces by the dry etching method. The tests were performed in pool boiling at atmospheric pressure by using FC-72 as the working fluid. The results showed that micro-finned surfaces could give a considerable increase in the boiling heat transfer as compared to smooth surfaces. In addition, the critical heat flux increased almost twice as compared to the smooth surface.

Therefore, the present work brings new perceptions of the microstructured surfaces in the boiling process and, consequently, in the HTC, making it possible to establish basic design guidelines for new surface technologies with high heat removal capacity for advanced applications in thermal management.

2. EXPERIMENTAL FACILITY

Figure 1 shows the pool boiling apparatus, which consists of a rectangular vessel made of glass. Inside the boiling chamber, in the upper part, there is a condenser cooled by water whose temperature is controlled by a thermostatic bath in order to control the saturation pressure inside it. An auxiliary heater – a cartridge resistance with a maximum power of 250 W at 220 V – submerged in the working fluid is used to maintain the liquid temperature near the saturation state.

Two K-type thermocouples, T_{liq} and T_{vap}, located in the liquid and vapor regions of the vessel, respectively, are used to monitor the test fluid temperature. An absolute pressure transducer Omega PXM309-2A measured the pressure inside the boiling chamber. The experiments were performed under conditions close to the local atmospheric pressure, p_{atm} = 98 ± 0.05 kPa.

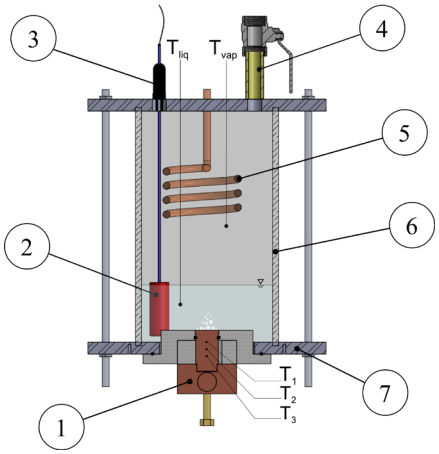

1) Cooper block;
2) Auxiliary heater;
3) Pressure transducer;
4) Feed Valve;
5) Condenser;
6) Glass chamber;
7) Stainless steel plate.

Figure 1. (a) Pool boiling apparatus: (1) cooper block; (2) auxiliary heater; (3) pressure transducer; (4) vacuum/feed valve; (5) condenser; (6) glass chamber; (7) stainless steel plate.

The test section consists of a copper piece with a square face at the top surface (16 × 16 × 3 mm^3) on a copper block with 16 mm diameter and 60 mm height; three K-type thermocouples (T_1, T_2, and T_3) with 0.5 mm diameters are used to estimate the wall temperature (T_w) and the heat flux ($q''_{measured}$). A cartridge resistance heats the bottom part of the copper block and the power is supplied by a stabilized variable DC power source. The thermal insulation of the test section consists of polytetrafluoroethylene (PTFE).

The boiling tests are performed by using deionized water (DI water) at saturation conditions. As a reference surface, it is used a plain surface (R_a = 0.14 μm) obtained by using the polishing method presented by Manetti et al. (2017). Vacuum is created to feed the chamber with the working fluid. Before each run, the auxiliary heater boils the working fluid during 1 hour for degassing it. The test conditions are adjusted by monitoring the pressure and the temperature inside the boiling chamber. For each test, the experiment is carried out at least twice under similar conditions to ensure that the results were repeatable.

A data acquisition system (Agilent 34970A) acquires all data signals (voltage, pressure, and temperature). The heat flux and surface temperature are calculated according to Fourier's Law assuming 1-D conduction based on the wall temperature measurements from the thermocouples in the copper block.

The HTC was calculated using Newton's law of cooling given by:

$$h = \frac{q''_{measured}}{T_w - T_{sat}\,(p_{int})} = \frac{q''_{measured}}{\Delta T_{sat}} \tag{1}$$

where $T_{sat}(p_{int})$ corresponds to the saturation temperature of the DI water at pressure inside de boiling chamber, and T_w is the wall temperature determined by extrapolating the linear temperature profile to the copper block upper surface.

Different linear temperature curve fittings, with R-square always higher than 0.99, were obtained for each heat flux based on the temperature measurements provided by the thermocouples embedded in the copper block. Figure 2 displays the temperature profiles and the curve fittings.

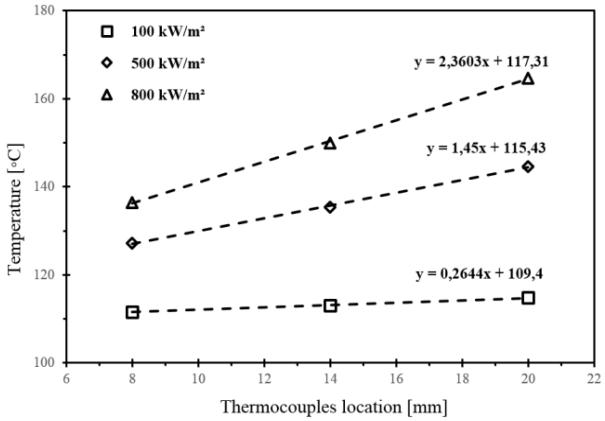

Figure 2. Example of linear temperature profiles used to estimate the heat flux and wall temperatures.

The assumption of negligible heat losses in the radial direction seems suitable; otherwise, a linear profile would not fit the experimental data. Moreover, Fig. 3 shows the comparison between the imposed heat flux and the heat flux estimated from the linear profile reveals heat losses always lower than 15%.

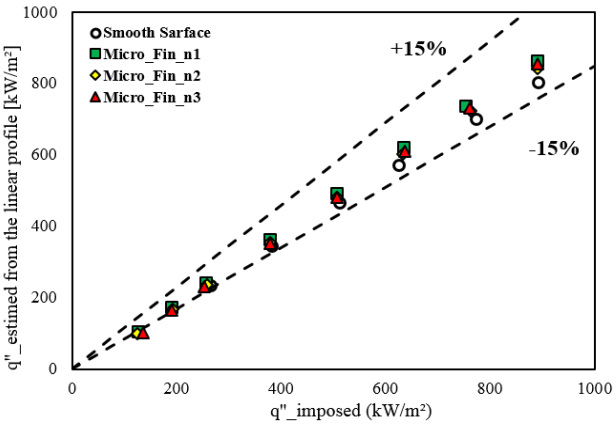

Figure 3. Comparison between the imposed heat flux and the heat flux estimated from the linear profile.

The experimental uncertainties are estimated by using the method described by Moffat (1988). For all surfaces tested, the experimental uncertainty for the heat flux and the heat transfer coefficient varied from 10.0 to 2.6 % and from 10.7 to 4.7 %, respectively.

The square-micro pillar arrays were etched on a plain copper surface through micro-milling process by using CNC precision machining. Squares micro-fins of different length scales (*i.e.,* height and diameter) were uniformly spaced on the plain copper surface. The inter-fin space had the same value, 250 μm, for all surfaces in order to control the effective roughness, *r*, defined as the ratio of the area in contact with the liquid to the projected area, as showed by Chu et al. (2012) and Dong (2014).

The droplet dynamic and wettability analysis consisted of the measurement of the static contact angle, θ, of a 10 μl DI water droplet by using a high-speed camera. Figure 4 shows the schematic layout used for this analysis

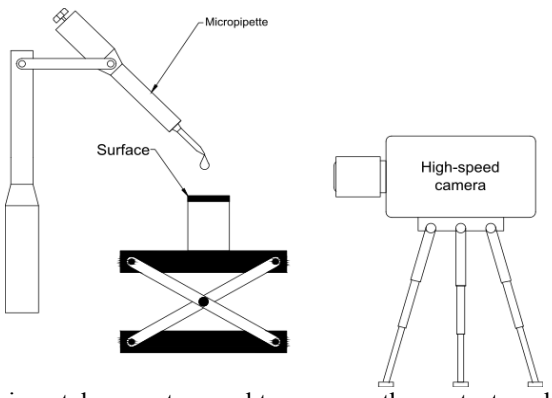

Figure 4. Schematic of the experimental apparatus used to measure the contact angle and to perform the wettability analysis.

The procedure adopted to evaluate the static contact angle consisted of depositing on the test surface a sessile droplet of DI water through a micropipette pointed vertically down onto the sample. Then, a camera captured the images of the droplet on the surface. After that, the pictures were analyzed using open source Java image processing program, ImageJ, to shape the deionized water droplet.

3. RESULTS AND DISCUSSION

Table 1 shows the scanning electron microscopy (SEM) images and the length scales of the micro-fin array surfaces tested. The micro-fin array has a good symmetry; the effective roughness, *r*, increases as the diameter or the height of micro-fins changes, being the height effect more pronounceable.

Table 1. SEM images of the micro-fin array surfaces.

SEM top surface image	Height [μm]	Diameter [μm]	Inter-fin space [μm]	Effective roughness, *r*	Number of fins
Micro_Fin_n1 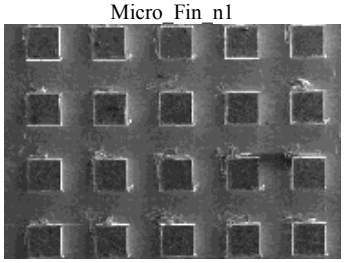	150	250	250	1.60	1024
Micro_Fin_n2 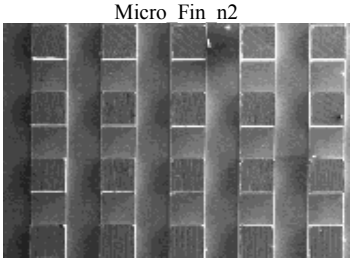	200	250	250	1.80	1024
Micro_Fin_n3 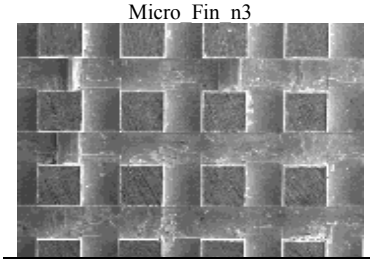	200	300	250	1.79	841

**Ratio of top surface area of micro-fins to the projected area of the sample.*

[1] $r = 1 + \left[\frac{4DH}{(S+D)^2}\right]$

Table 2 shows the DI water droplet dynamic and surface wettability for all surfaces. In addition to the modified surfaces, we also tested a plain surface (corresponding to a copper surface with R_a = 0.14 μm) as a reference surface.

Table 2. Wettability results and their respective contact angles.

Surface	Wettability	Static contact angle, θ_y
Plain Surface	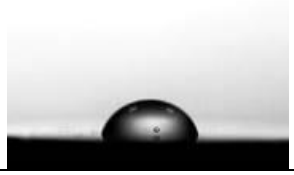	95°

Micro_Fin_n1	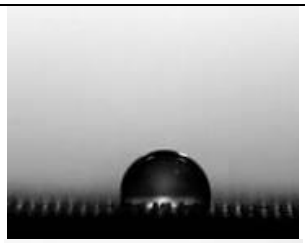	107°
Micro_Fin_n2	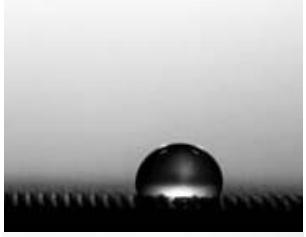	111°
Micro_Fin_n3	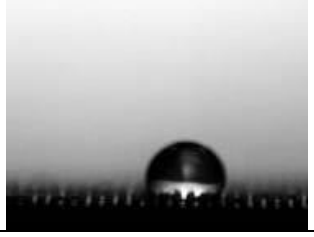	115°

The plain and micro-fins showed low wetting behavior. This effect is due to the micro spacing in the micro-fins array surface. As a result of non-wetting surface behavior, the promising nucleation cavities are not flooded with the liquid, allowing the trapping of vapor which contributes to the activation of the nucleation sites and, consequently, to an increase in heat transfer.

The boiling heat transfer behavior for DI water at saturated conditions is presented in Fig. 5. One may observe that the micro-fin surfaces intensify the HTC as compared to the plain/smooth surface. The surface thermal behavior is a function of the surface morphology and its surface wettability and capillary wicking.

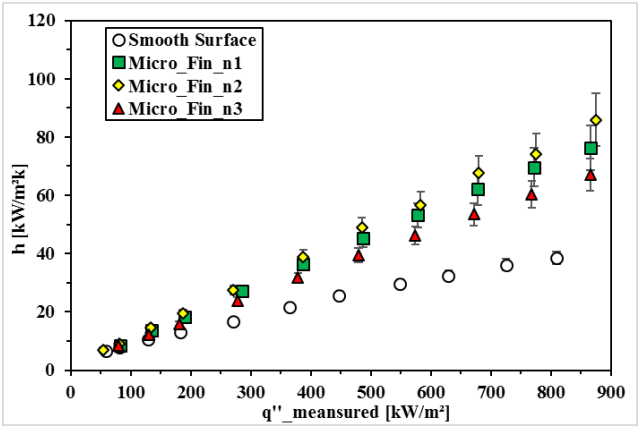

Figure 5. HTC curve of all surfaces tested and for DI water at saturated conditions.

In order to understand the heat transfer mechanism, Figure 6 shows the micro-pillars parameters that can influence the boiling heat transfer. The presence of the micro-fins increases the heat exchange area (the area in contact with the liquid), leading to an increase in the heat transfer coefficient as compared to the flat surface. From the parameters analyzed in this study, the number of pillars seems to be the main factor for the HTC enhancement (‘Micro_Fin_n1’ and ‘Micro_Fin_n2’, both with 1024 micro-pillars, have higher heat transfer coefficients than ‘Micro_Fin_n3’, with 841 micro-pillars).

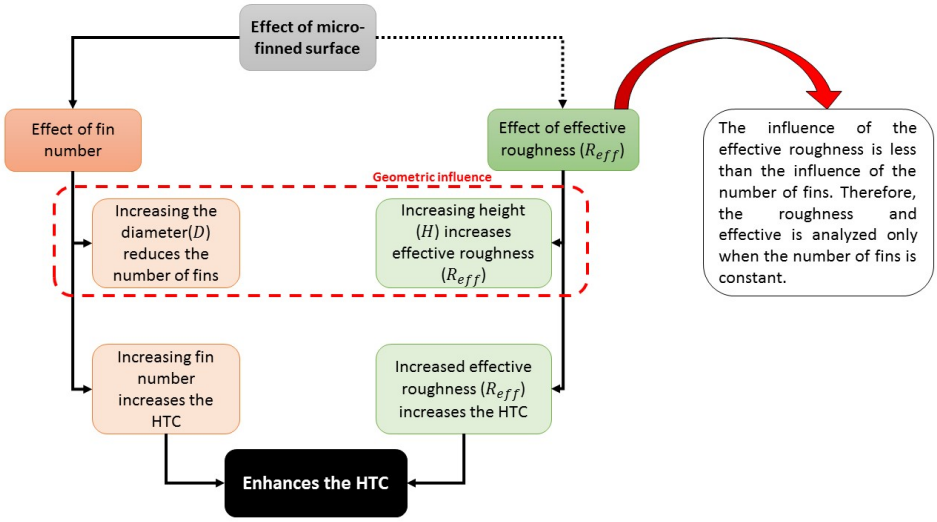

Figure 6. Micro-finned surface parameters effect on heat transfer pol boiling.

However, if the numbers of micro-pillars are constant, it is necessary to analyze the effective roughness or roughness factor, defined by the relation between the surface area and the projected area; thus, the larger the effective roughnesses the higher the heat transfer performance.

In order to show more clearly the effect of the micro-fin surfaces on the enhancement/deterioration of the HTC, the experimental results were evaluated using the heat transfer enhancement ratio ($h_{HTE} = h_{Fin}/h_{Plain}$), where h_{Fin} is the heat transfer coefficient for the micro-fin surfaces, and h_{Plain} is the HTC for the plain surface. In Fig. 7, the h_{HTE} increases with increasing heat flux and number of micro-pillars on the heating surface.

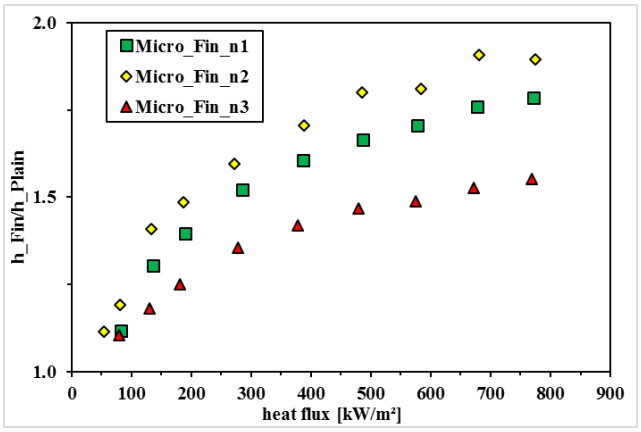

Figure 7. Pool boiling heat transfer coefficient enhancement ratio as a function of heat flux, for all surfaces tested.

Bubbles dynamics were visualized by using a high-speed camera (Photron FASTCAM SA3 with a Tokina MACRO 100 mm lens) with 1024 × 1024 maximum resolution and 1000 fps. Through videos and image tracking software, the bubble diameter, and frequency could be analyzed qualitatively after the instant time that the bubble detached from the surface, Fig. 8.

	75 [kW/m²]	100 [kW/m²]	300 [kW/m²]	500 [kW/m²]
Plain	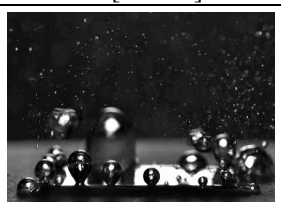	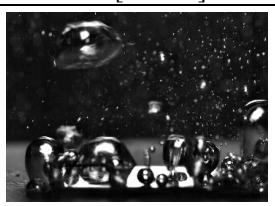	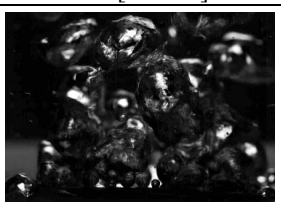	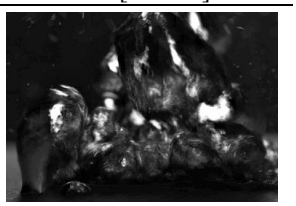
	ΔT_{sat} = 9.02 ºC	ΔT_{sat} = 10.6 ºC	ΔT_{sat} = 16.2 ºC	ΔT_{sat} = 17.5 ºC

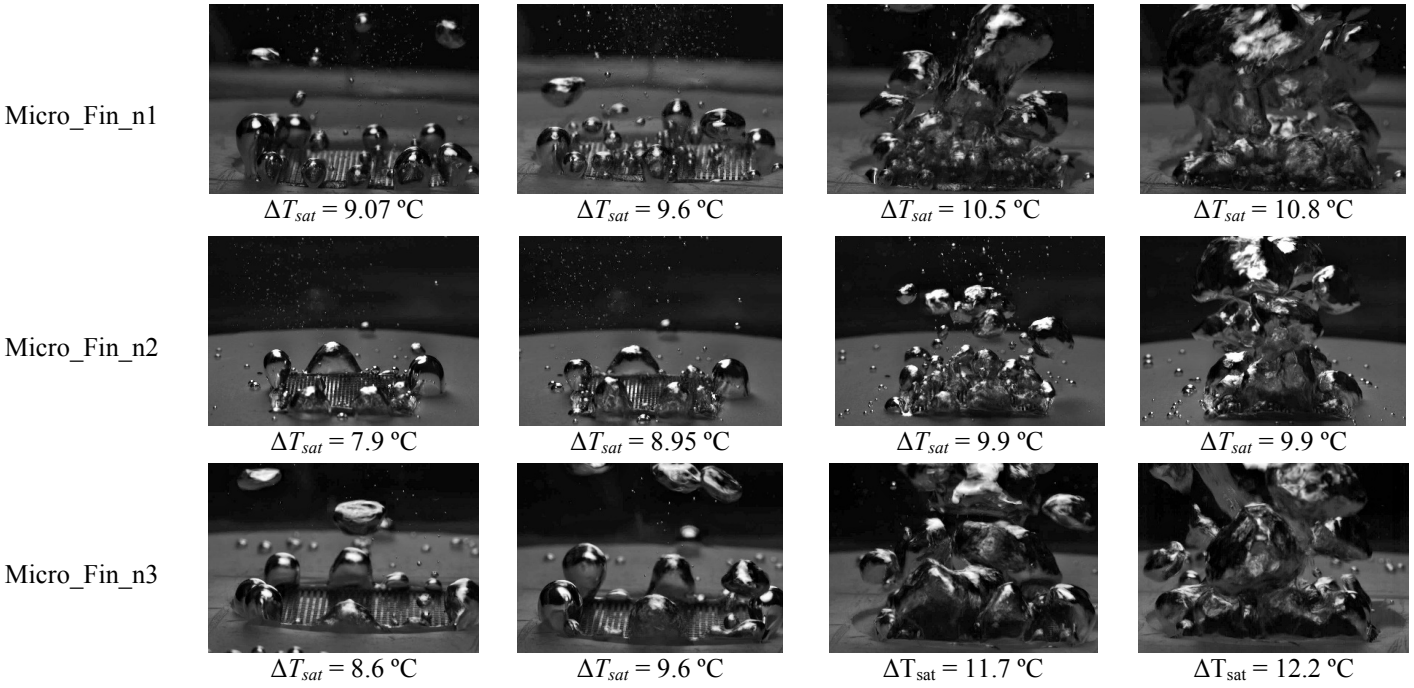

Figure 8. Vapor bubbles visualization for different heat fluxes for plain and micro-fins surfaces.

For lower heat fluxes, there is the coexistence of isolated and coalesced bubbles, as shown in Fig. 8. Under this condition, there is still a gap between the bubbles and the natural convection predominates as heat transfer mechanism. As heat flux increases, the wall superheating is lower for the micro-fins surfaces as compared to the plain one, indicating an improvement in the heat transfer performance.

4. CONCLUSIONS

Based on the analysis, the HTC enhancement by using micro-fins surfaces is related to the number of fins on the heated surface, to the effective roughness and to the wettability. The presence of the micro-fins increases the heat exchange area (the area in contact with the liquid), leading to an increase in the heat transfer coefficient as compared to the flat surface. Moreover, due to non-wetting surface behavior the promising nucleation cavities are not flooded with the liquid, allowing the trapping of vapor which contributes to the activation of the nucleation sites and, consequently, to an increase in heat transfer.

5. ACKNOWLEDGEMENTS

The authors are grateful for the financial support from CAPES, from CNPq (458702/2014-5) and from FAPESP (2013/15431-7, 2017/13813-0 and 2019/02566-8). The authors also extend their gratitude Prof. Alessandro Roger Rodrigues from EESC/USP for his important contribution in this work.

6. REFERENCES

Bejan, A.,1984. "*Convection heat transfer*", John Wiley & Sons, Nova York.

Cao, Z., Liu, B., Preger, C., Wua, Z., Zhang, Y., Wanga, X., Messing, M. E., Deppert, K., Wei, J., Sundén, B., 2018. "Pool boiling heat transfer of FC-72 on pin-fin silicon surfaces with nanoparticle deposition" *International Journal of Heat and Mass Transfer,*Vol. 126, pp. 1019 – 1033.

Chu, K-H., Enright, R., and Wang, E. N., 2012. "Structured surfaces for enhanced pool boiling heat transfer." *Applied Physics Letters*, Vol. 100, n. 24, p. 241603.

Demir, E., Izci, T., Alagoz, A.S., Karabacak, T., Kosar, A., 2014. "Effect of silicon nanorod length on horizontal nanostructured plates in pool boiling heat transfer with water." *International Journal of Thermal Sciences*, Vol. 82, pp. 111-121

Dong, L., Xiaojun Q. and Ping C., 2014. "An experimental investigation of enhanced pool boiling heat transfer from surfaces with micro/nano-structures." *International Journal of Heat and Mass Transfer,* Vol. 71, pp. 189-196.

Dong. L., quan, X., cheng, P., 2014. "An experimental investigation of enhanced pool boiling heat transfer from surfaces with micro/nano-structures", *International Journal of Heat and Mass Transfer*, v.71, pp. 189-196.

Liang, G.; Mudawar, I. 2019. "Review of pool boiling enhancement by surface modification." *International Journal of Heat and Mass Transfer*, Vol. 128, pp. 892-933

Manetti, L.L., T. S. Mogaji, T. S., Beck, P. A., Cardoso, E. M., 2017. "Evaluation of the heat transfer enhancement during pool boiling using low concentrations of Al2O3 -water based nanofluid", *Exp. Therm. Fluid Sci.* Vol.87, pp.191–200.

Nirgude, V.V.; Sahu, S, K., 2017. "Enhancement of nucleate boiling heat transfer using structured surfaces." *Chemical Engineering & Processing: Process Intensification*, Vol.122, pp.222-234.

7. RESPONSIBILITY NOTICE

The author(s) is (are) the only responsible for the printed material included in this paper.